applied sciences

MDPI

Article

Blasting Fragmentation Study Using 3D Image Analysis of a Hard Rock Mine

Janine Figueiredo [1], Vidal Torres [2], Rodolfo Cruz [3] and Douglas Moreira [2,*]

[1] Vale S. A., Porto de Tubarão, Vitória 29090-900, ES, Brazil; Janine.Figueiredo@vale.com
[2] Instituto Tecnológico Vale, Ouro Preto 35400-000, MG, Brazil; Vidal.Torres@itv.org
[3] Vale S. A., Serra do Esmeril, Itabira 35900-900, MG, Brazil; Rodolfo.Matias@vale.com
* Correspondence: Douglas.Moreira@pq.itv.org

Abstract: Rock blasting with explosives is the first stage of rock fragmentation and plays a key role in the results of the mining chain. Fragmentation optimization is achieved by considering the energy efficiency of the explosive, the optimal distribution of explosive energy in the rocky mass, and the programmed and controlled release of explosive energy during blasting. The quality of fragmentation is usually performed using tools that estimate the sizes of fragments via the analysis of two- or three-dimensional images. This article presents a study of the rock fragmentation optimization of very compact itabirites, based on four blasting tests, performed in a different way from the conventional blasting design. The fragmentation analysis was performed using the PortaMetrics^{TM} tool, and compared with the Kuznetsov and Rosin–Rammler particle size distribution model, to compare the reliability of this tool. Finally, the mine productivity after blasting was estimated from the particle size distribution obtained in the tests. The model presented idealistic results considering the technical parameters used in the equations. However, the PortaMetrics^{TM} tool suggests good performance for the preliminary evaluation of blast design.

Keywords: 80% passing size; blasting design; very compact itabirite; mining productivity

Citation: Figueiredo, J.; Torres, V.; Cruz, R.; Moreira, D. Blasting Fragmentation Study Using 3D Image Analysis of a Hard Rock Mine. *Appl. Sci.* **2023**, *13*, 7090. https://doi.org/10.3390/app13127090

Academic Editor: Arcady Dyskin

Received: 10 May 2023
Revised: 6 June 2023
Accepted: 8 June 2023
Published: 13 June 2023

1. Introduction

The blasting of rocks using explosives is performed to fragment rocky material into blocks and particles of different sizes. In addition, the sizes of fragments must be smaller than those of the feeding of primary crushing [1,2]. Therefore, the optimization of drilling and blasting is essential for controlling ore fragmentation and, consequently, the productivity and operating cost levels of the subsequent stages. On the one hand, increasing fragmentation quality increases drilling and blasting costs; on the other hand, it reduces the costs of loading and hauling [1,3]. Therefore, the qualities of drilling and blasting activities are essential for generating adequate and uniform fragmentation for mining operational processes. Planning and executing these activities well leads to the effectiveness of breaking rocks into smaller blocks. When drilling, some parameters, such as the state of the rock mass, conditions of the floor and toe of the drilling bench, environmental factors, and missed holes [1], can interfere with the result of blasting via explosives.

With drilling and blasting techniques, despite being continuous and effective in a mining environment, in order to fragment the rock mass, fragmentation generates adverse impacts such as soil vibration, flyrock, dust, and noise [4,5].

Drilling and blasting continue to be deprecated techniques in relation to the fragmentation of rock masses, mainly aiming at possibilities for economic gains and productivity in the performance development sector. When observing the fragmentation of rock masses, these are observed with the possibility of fragmentation with generally a maximum of 30% of explosive energy and about 70% of losses in residues, with a negative influence from a safety perspective [6]. This approach can be better observed in techniques recently used in induced computational modeling for fragmentation analysis, in situations where there is

the possibility of using artificial neural networks, for example [4,6]. Via the use of neural networks, it is possible to delimit and optimize the fragmentation induced by explosives, whereby, according to several bibliographies, studies about these analyses are difficult to find [6].

It is worth mentioning that blasting via explosives presents events of positive and negative impacts, and through the execution of planning, and when executing it, it tends to fragment the rock, through the development of cracks in the surrounding rock and the release of heat, energy, pressure, and stress waves [4]. The mishandling of these explosives can generate undesirable effects such as overpressure, ground vibration, flyrock, noise, heat, dust, and counter-resistance [4]. Through the development carried out by several researchers, mainly due to flyrock, the relationship between the maximum distance of this parameter as a function of the hole diameter, shape, and velocity coefficient of the rock to be dismantled was observed. Figure 1 presents a schematic summary of the drilling and blasting operations.

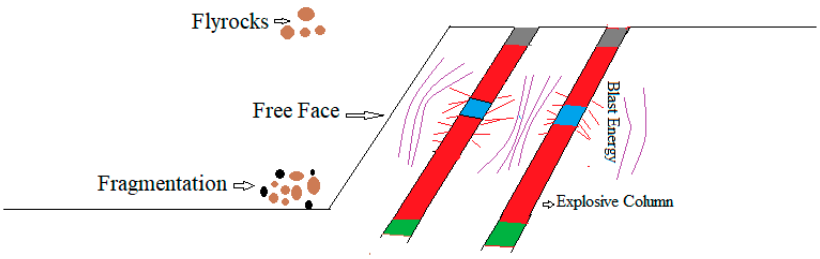

Figure 1. Schematic representation of operations during blasting.

Given the observations in Figure 1, the complexity of the analysis on the experimental procedures according to the blasting is verifiable, being the necessary techniques that help to gain a better perspective of the process, as is the case for the generated fragments. In this case, the fragmentation generated can be improved and optimized by observing the parameters used and via evaluation using the fragmentation model, generated by software, as in the case of PortaMetrics.

During blasting via explosives, material fragmentation can occur due to the formation of new fractures, the presence of in situ blocks that must be released from the rock mass, or the fragments generated by the extension of the in situ fractures combined with the new fractures [4]. By considering the energy efficiency of the explosive, during the explosion, the rock mass is fractured by high-pressure gas, causing a tensile stress field and the formation of cracks that develop and expand, thus rupturing and breaking the rock [5]. The application of a suitable explosive should be considered according to the rock's tensile stress and uniaxial compressive strength to fracture and fragment the rock into blocks of suitable sizes. In addition, the fragmentation of the rock mass directly influences the operating costs, observing the calibration of transport, crushing, excavated materials, and other processes [6].

The programmed release and control of explosive energy during blasting is performed by adjusting the departure angle at the detonation of the explosive charge. This angle is determined by the relationship between the burden and spacing; consequently, the explosive energy and the level of fragmentation of the rocks are controlled by adjusting these parameters [7,8]. Additionally, the hole diameter determines the mesh size (burden x spacing); therefore, for holes with smaller diameters, smaller spacings generate smaller fragment sizes than blasts with larger hole diameters and spacings.

To contribute to fragmentation optimization, in blast planning, some parameters can be modified, such as the hole diameter, spacing, explosive amount, explosive type, stemming material size, and type [3,9].

The quality or degree of fragmentation of blasting has been evaluated by indicators of blasting performance, such as the granulometric distribution of the blasting material [1,10–12], the excavation time and productivity of shovels [13–15], and the loading time

of trucks, by the truck hauling time over short distances, by the hauling productivity, or by the productivity of primary crushing [10,11,16].

The evaluation of blasting fragmentation by defining the particle size distribution curve has been performed via image analysis using equipment and software available on the market, such as Split-Desktop [1,12,15], WipFrag [2,17,18], and Fragblast PortaMetrics™ [17–20]. These technologies have no limitation on the sizes of the samples that can be analyzed. The errors inherent to the method can be minimized by capturing many high-quality images for analysis [2]. Some of these methods require the use of a scale object to help determine the sizes of the fragments, which may require the presence of humans in the field and may not be the safest alternative. Some methods have better data processing than other equipment available on the market, providing immediate and accurate fragmentation analysis [18].

A well-known example of the distribution of rock fragmentation analysis, known as RFD, is currently widely used in order to simulate and optimize drilling and blasting operations, with this movement being reflected even in the primary stages of crushing. An example is the operations of the Sarcheshmeh copper mine [1]. It is worth mentioning that the increase in the amount of material to be fragmented increases the cost of drilling and reduces loading and transportation costs. However, there are problems that can be generated from the definition of mining to be adopted, such as the need for secondary and even tertiary blasting [1,17,18].

According to [1], when using Split-Desktop software, seeking the analysis of fragmentation using the RFD method, five steps are necessary, which are image dimensioning, the automatic or manual limitation of the fragments, the estimation of fines, the evaluation of the results, and the export of the analysis result to a Kuz–Ram curve plotted in Excel, demonstrated in the work performed by the same authors, with an d80 of 13.06 cm and a d50 of 6.48 cm, post-blasting. In the work developed using the same method in [12,15], it was possible to delimit the effectiveness of the method in the dismantling carried out, analyzing the size of the fragment and the effect of loading through the operational variables. It was possible to observe that the Kuz–Ram method, for such a methodology, overestimated the RFD from coarser granulometry and underestimated the fine granulometry.

In addition, the Split-Desktop method involves at least five steps, which are considered to be the following: sizing the image, segmenting the fragments, the possibility of editing the fragments, analyzing the marked parts, and the distribution diagram of size [4].

Another technique that is widely used is the analysis of fragmentations via WipFrag with the help of the empirical model of Kuz–Ram. In the work developed by [2], when developing a project for the evaluation and optimization of blasting, images captured from a Muck pile were used. The results obtained by the method can vary significantly; therefore, three tests were carried out, and all of which presented satisfactory and similar results. However, it is worth noting that the Kuz–Ram model presents idealistic results due to the variation in rock characteristics, being widely used for the preliminary assessment of blasting [2].

When describing the operation of the equipment [17,18], a post-dismantling 2D camcorder is used to record images of the dismantled pile. For the record to be conducted efficiently, photos must be taken from different angles, and the image must be transformed into a fragmentation map. This equipment is considered to be good for more superficial analyses, mainly generated via underground mine dismantling, with the possibility of using PortaMetrics as a more efficient method for open pit mining [18].

The objective of this study is to analyze the fragmentation results of very compact itabirites based on variations in some blasting design parameters for materials with high-strength geotechnical and geomechanical characteristics. Fragmentation is studied by defining the particle size distribution of the blasting material through monitoring images using the PortaMetrics™ tool. Finally, the impact of fragmentation resulting from blasting on the productivity of mining operations is estimated.

It is worth noting that, currently, the application of technological analysis via machine learning techniques, such as neural networks, has grown abruptly in mining, and previous studies of dismantling such as the one performed in this article are indicated, in order to enable the development of new approaches to the subject [4]. Such approaches can assess, for example, the quality of the blasting in terms of the explosive materials used, thus generating a new study perspective.

2. Materials and Methods

2.1. PortaMetrics™ Image Capture

The second phase of the study consisted of analyzing the sizes of rock fragments obtained in blasting tests using images. A robust technology based on machine learning and image processing was used for fragmentation analysis: PortaMetrics™, equipment for capturing images in three dimensions (3D), and the image-processing platform MetricsManager™ Pro (MMPro).

PortaMetrics™ is a safe handheld device because it can accurately calculate rock fragmentation from a distance via stereo images. With this device, there is no need for mine technicians to be near the bench to place the object to scale. The stability of the bench face can be evaluated using the integrated inclination sensor, indicating the inclination angle and the distance to the bench face [19].

The equipment had three integrated high-resolution cameras (Figure 2) with a touch screen. Table 1 presents the main functions of the equipment.

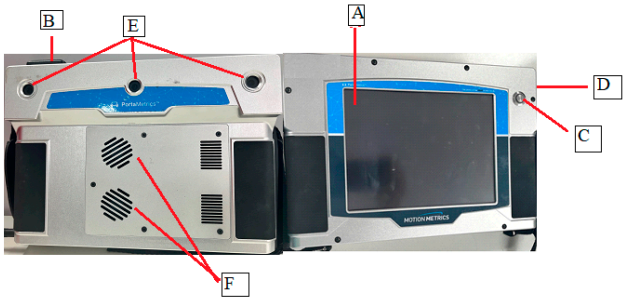

Figure 2. PortaMetrics™ equipment is used to capture 3D images.

Table 1. Each component of the PortaMetrics™ equipment and its function.

Component	Function
A: Touch screen	Edits and selects images
B: GPS antenna	Provides positioning information
C: Capture button	Captures/records the fragmentation for analysis
D: On/off button	For turning the equipment on and off
E: Cameras	Three stereoscopic cameras that create and analyze 3D fragmentations
F: Fan	Provides cooling to the equipment, preventing damage from overheating

Image capture was performed manually by pointing and shooting the device to the blasting pile, with the least amount of disturbance in the environment (dust, vibration, and shadow). It was recommended to capture images in the morning to avoid shadows. The three cameras could detect the distance from the user to the fragments to calculate the size. The application had a NEAR/FAR mode disparity sensor, where the NEAR mode was for distances less than or equal to 2.00 m, the FAR was for distances longer than 2.00 m and shorter than 10.00 m, and the size of the smallest detectable particle was 0.03 m. Users had to adjust the region of interest to cover, at most, 80% of the screen [19] and capture an image, and the results were instantly displayed in an intuitive graphical user interface of the portable device.

2.2. PortaMetrics™ Image Analysis

After capturing the images, an artificial intelligence algorithm named Fragmentation Artificial Intelligence (FMAI) performed the processing and thus provided a precise image of the captured region of interest (ROI). The data obtained were sent to the MetricsManager™ Pro platform, displaying the same data in the cloud, allowing the fragmentation results to be shared remotely. In this platform, the user could view each image with date, time, and location information because the captured images were associated with the specific location of the blasting site with an integrated global positioning system (GPS) [19].

In the MetricsManager™ Pro platform, there were resources for manual correction to help the automatic analysis function and improve the results. It was possible to adjust the images, such as adjusting the ROI, manually joining or dividing rock fragments, delimiting the fines region, and delineating a fragment that was not automatically detected. Editing tools were used to improve the detection of fragment boundaries. The processes were repeated for other images in the same blast stack. The algorithm used to determine the fragment size considered the longest dimension of the rock and its shape factor [18]. Finally, with the measurement of the sizes of the blocks and particles, the distribution curve of the percentage pass and the table of cumulative sizes were generated for each image.

The images were chosen to create reports that included certain information, such as the average parameter in which 80% of the material passed through the sieve the particle size distribution curve, the statistical frequency of size, the location, and the slope measurements of the face of the bench [19].

In order for the PortaMetrics analysis to occur in a justified manner, its activity sequencing must have been previously detailed with maximum precision, to the point of validating how the equipment performs in the face of an investigation. To this end, the sequencing of the activities governed by it is based primarily on capturing the fragmentations with a tablet with 3 cameras available and the possibility of investigating the 3D analysis. After that, the model can be calibrated with the operator handling the equipment, or even in the software portal, where the fragmentation images are inserted via the digital cloud. With regard to these parameters, being delimited and sequenced according to the desired granulometry, some requirements must be respected, such as avoiding the presence of shadows and respecting the granulometry and distance limits, which are considered to be 32.81 feet in distance and a minimum granulometry of 1.18 inches. At the end, the fragmentation curve obtained manually via two models, the Swebrec and the Kuz–Ram model, becomes available, with the latter being selected for comparisons in this work in the equipament PortaMetrics.

A well-known and used technique in comparison to PortaMetrics is WipFrag, whereby, as seen in Figure 3, it appears that despite the precision presented by the device, it needs the support of an object for delimitation and the use of a measurement parameter, which is not needed in PortaMetrics [21].

So that the visualization of the operationalization was mostly evidenced, operational sequencing of the post-blasting PortaMetrics was carried out according to Figure 3. It is worth noting that the entire operation was recorded right after the primary dismantling, with Figure 3 being highlighted as a flowchart, thus leaving the operating mode of the equipment as perceptible.

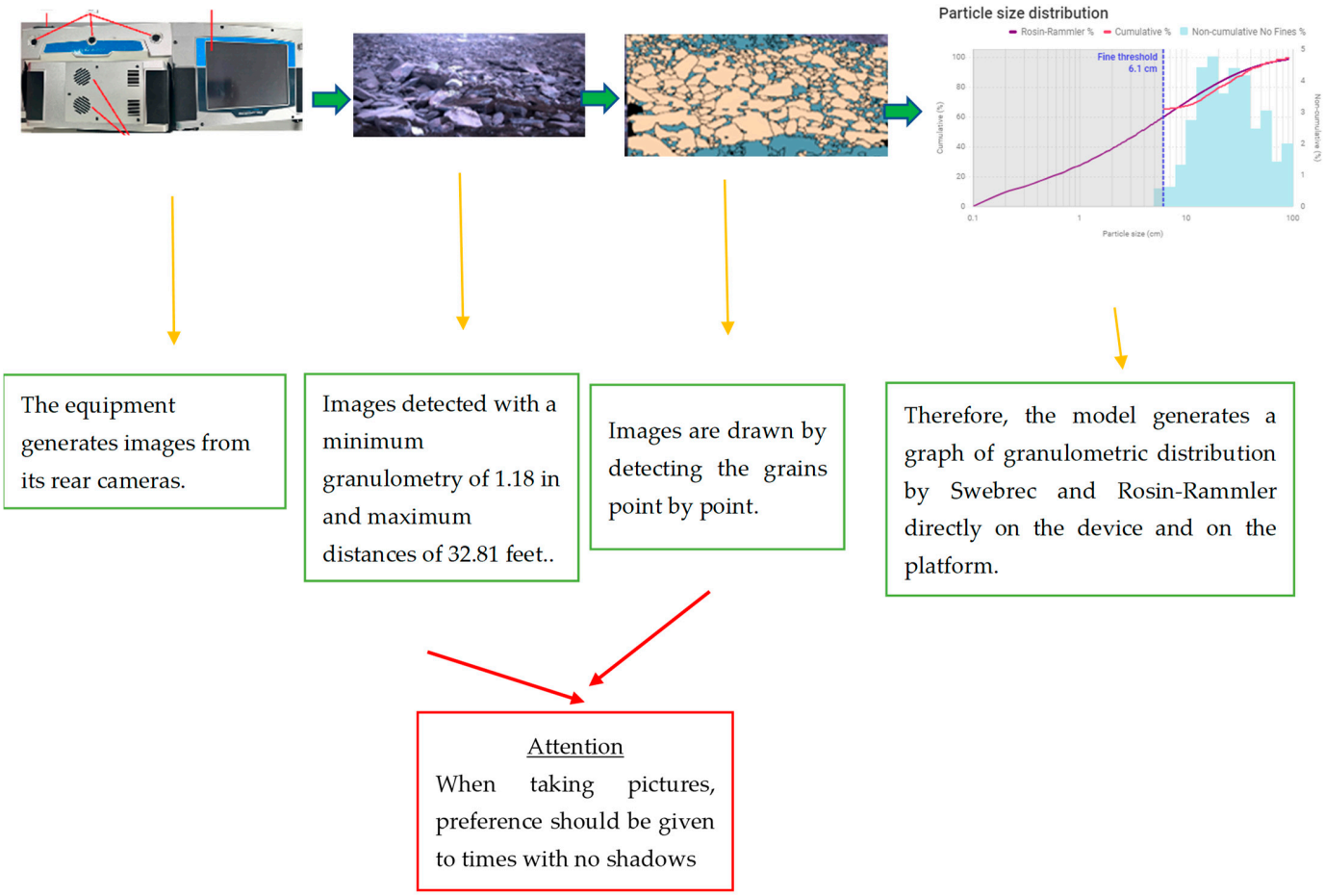

Figure 3. Flowchart of equipment operation.

2.3. Kuz–Ram Model Analysis

The particle size distribution of the blasting fragments considered the average size of the blocks generated (X_{50}) and the uniformity index (n). The Kuz–Ram model was used to predict the particle sizes of the fragments resulting from the blasting tests proposed in this study.

The Kuz–Ram model considered three equations: the modified Kuznetsov equation (Equation (1)), first developed by Kuznetsov [20] and modified by Cunningham [22–24]; the Rosin–Rammler equation (Equation (2)) [25], and the Cunningham uniformity index (n) equation (Equation (3)) [26]. It is worth noting that the K-factor is also known as the powder factor, that is, the necessary factor for evaluating the rock fragmentation power in the desired granulometry.

$$X_{50} = A_r K^{-0.80} Q^{0.167} \left(\frac{115}{RWS}\right)^{0.633} \quad (1)$$

where X_{50} (cm) is the average size at which 50% of the particles pass the sieve; A_r is the characteristic factor of the rock [27]; K (kg/m^3) is the loading ratio; Q (kg) is the mass of explosive per hole; and RWS (%) is the relative power by weight of the explosive relative to the energy of the ANFO (115 is the RWS of the trinitrotoluene (TNT) [24]).

The Rosin–Rammler equation (Equation (2)) estimated the complete fragmentation distribution using the percentage of retained fragments [26] for a sieve opening size:

$$P(x) = 1 - e^{-\left(\frac{X}{X_c}\right)^n} \quad (2)$$

where $P(x)$ is the cumulative frequency passing (%) through the opening of the sieve of size X; X (cm) is the size of the sieve opening; and X_c (cm) is the characteristic size. The characteristic size is the size at which approximately 63.20% of the material passed through [28], and it could be obtained using the following equation:

$$X_c = \frac{X_{50}}{(0.693)^n} \quad (3)$$

By defining the uniformity index using Equation (4), it was possible to prepare the particle size distribution curve [22,23]:

$$n = \left[2.20 - 14\left(\frac{B}{D}\right)\right] \cdot \sqrt{\left[\frac{\left(1 + \frac{S}{B}\right)}{2}\right]} \cdot \left[\left(1 - \frac{W}{B}\right)\frac{L}{H}\right] \cdot \mathrm{P} \quad (4)$$

where B (m) is the burden; D (mm) is the diameter of the hole; S (m) is the spacing; W (m) is the standard deviation of the perforation; L (m) is the height of the explosive charge; H (m) is the height of the bench; and P is the perforation factor for stepped loading, which is equal to 1.10 [2,26].

2.4. Blasting Design Tests

The first stage of this study consisted of the development of a test design for blasting with explosives to improve the quality of fragmentation of very compact itabirites, which would be compatible with the maximum opening of the primary crusher, that is, equal to 1.20 m. This study was needed because the lithologies of the mine had high-density and simple compressive strength (CUS) values; additionally, there was a need to control the generation of large fragments, which were incompatible with the maximum size of the primary crusher feed. The geomechanical characteristics of the studied lithology are presented in Table 2.

Table 2. Geomechanical characteristics of the HCI.

Properties	Values
Density (kg/m ^{3})	3.300
P wave velocity (m/s)	4.308
Simple compressive strength (MPa)	350
Tensile strength (MPa)	33
Young's modulus (GPa)	47
Poisson's coefficient	0.22
Protodyakov's coefficient	13
Diving lithology (°)	60

The design of blasting tests, in very compact itabirites, considered holes with diameters of 250.80 mm. The explosive used had a density of 1250 kg/m^3, velocity of detonation (VOD) between 3500 and 6000 m/s, and relative power strength (RWS) of 97% relative to ammonium nitrate fuel oil (ANFO). The accessories adopted were a 0.90 kg booster and an electronic fuse for sequencing the detonation of 7 ms between holes and 60 ms between lines. In total, 4 tests were performed by considering modifying the parameters of the blasting design using explosives, and, via comparison, a blasting test was conducted by considering the conventional parameters used in the mine. Table 3 presents the parameters of the blasting tests performed. In this table, the parameters to be investigated according to the tests are B (m) as burden, S (m) as spacing, RC (kg/m^3) as charge ratio, H (m) as bench height, L (m) as explosive charge length, St (m) as stemming, Q (kg) as number of explosives per hole, and J (m) as sub-drilling.

Table 3. Mean parameters of the blasting tests performed in HCI.

Blasting	No. of Drills	H (m)	B (m)	Y (m)	L (m)	St (m)	J (m)	Q (kg)	Rc (kg/m^3)
Test 1	24	15.00	4.00	4.80	10.14	5.65	0.79	668	2.06
Test 2	48	16.00	4.00	5.00	12.40	3.96	0.36	776	2.49
Test 3	36	15.00	4.00	5.00	11.43	4.21	0.64	701	2.59
Test 4	35	16.00	4.20	5.40	11.94	4.00	0.00	714	1.98
Conventional Test	114	16.00	4.20	5.40	11.94	4.00	0.00	713	1.46

In a conventional test, the holes were loaded in a staggered manner with 600 kg of explosives and a deck with a blast bag, and the second load included approximately 150 kg of explosives and buffer.

2.5. Impacts on Mine Productivity

An analysis of the impacts of blasting tests performed on the productivity levels of the phases after blasting was performed regarding the relationship between the blasting particle size distribution and the estimate of productivity for each stage: loading, hauling, and primary crushing.

The mine-to-crusher methodology was used to increase productivity and reduce operating costs from the mine to the primary crusher or crusher [1,3,28–30], based on the blast fragmentation parameter X_{80}. In this study, the equations presented in Navarro Torres et al. [3], which were adapted for the present case study (Table 4), were used to estimate the productivity of each phase of mine operation.

Table 4. Productivity equations for the drilling and blasting, loading, transport, and primary crushing phases.

Productivity (t/h)	Variables
$P_c = U_c \frac{3600 L_c}{a\left(exp^{0.05X_{80}}\right)+2t_{sw}+t_d}$	P_c: loading productivity; U_c: physical use of the excavator (%); L_c: excavator payload; a: lithology calibration coefficient; t_{sw}: turnaround time (s); and t_d: discharge time (s).
$P_t = U_t \frac{60 L_t}{\left[a\left(exp^{0.05X_{80}}\right)+2t_{sw}+t_d/60\right]p+\left(t_v+t_f\right)}$	P_t: transportation productivity; U_t: physical use of transport (%); L_t : average transport load (t); p: number of passes; t_v: variable time (min); and t_f: fixed time (min).
$P_{bpX_{80}} = P_{bp} e^{-0.002X_{80}}$	$P_{bpX_{80}}$: primary crushing productivity and P_{bp}: real productivity (t/h).

3. Results and Discussion

The results of the particle size analysis of the piles of fragmented material from the five blasting tests, obtained using the MMPro platform, were compared with the particle size distribution curves obtained using the Kuz–Ram model, as shown in Figure 4A–E. This configuration is presented graphically using a logarithmic scale for a better perception of the results presented by blasting.

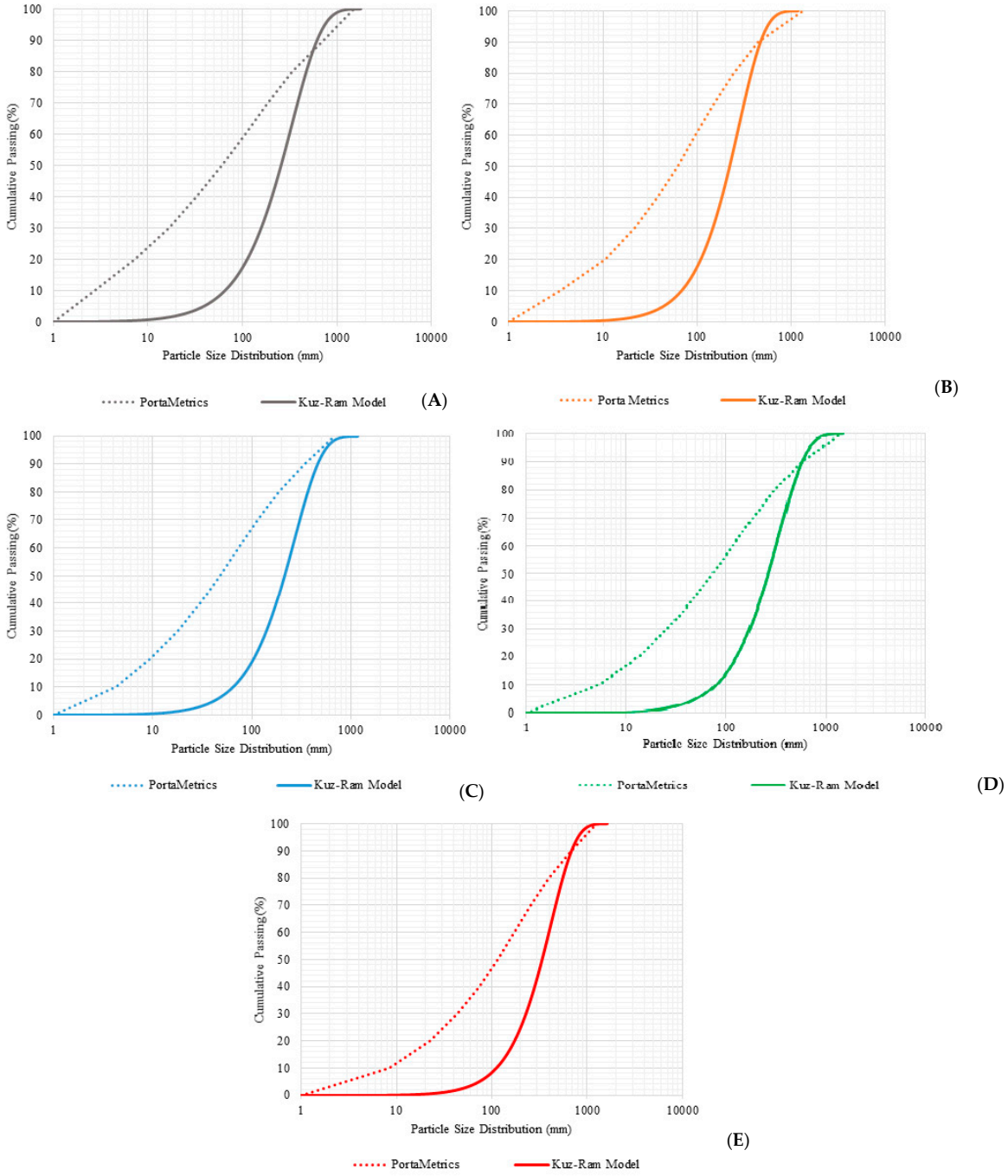

Figure 4. Kuz–Ram and MMPro particle size distribution for (**A**): Test 1, (**B**): Test 2, (**C**): Test 3, (**D**): Test 4, and (**E**): conventional test.

Through the analysis of the particle size distribution curves and Table 5, the Kuz–Ram model for Tests 1–3 with new blasting designs shows that the size at which 80% of the fragments pass through (X80) should be approximately between 365 and 469 mm; for Test 4 and conventional blasting, the X80 values would be 457 and 556 mm, respectively. By considering the values measured using the MMPro platform, it was found that for conventional blasting, the X80 value was 398 mm, and for Test 4, it was 305 mm. Thus, it was understood that the proposal of a smaller blasting pattern led to better fragmentation since the values of X80 were lower for Tests 1–3, correctly planning the configuration of the blasting parameters and optimizing the fragmentation of the blasting parameters of very compact itabirites. Additionally, Test 4 was performed with a pattern of the same size as

conventional blasting with an increased load ratio. The results showed improvement in fragmentation relative to conventional blasting of the same pattern made with staggered explosive loading.

Table 5. Parameters obtained using the Kuz–Ram model and the PortaMetrics platform.

Parameter		Tests				
		1	**2**	**3**	**4**	**Conventional**
n	Kuz–Ram model	1.37	1.58	1.56	1.54	1.69
	PortaMetrics	0.48	0.61	0.51	0.52	0.36
X_c (mm)	Kuz–Ram model	331.46	281.44	269.19	335.72	419.48
	PortaMetrics	125.86	111.00	82.83	134.00	194.92
X_{50} (mm)	Kuz–Ram model	253.44	223.28	212.73	264.52	337.45
	PortaMetrics	60.29	61.91	47.08	74.00	114.42
X_{80} (mm)	Kuz–Ram model	469.19	379.80	365.14	457.12	556.01
	PortaMetrics	341.29	242.82	186.00	304.76	398.08
X_{100} (mm)	Kuz–Ram model	1775.00	1198.00	1175.00	1492.00	1637.00
	PortaMetrics	1530.00	1319.36	686.33	1421.86	1252.08

By observing the particle size distribution curves of Figure 5, it was found that the particle size distribution curves of the Kuz–Ram model were slightly different from the particle size distribution curves generated in the MMPro platform of PortaMetrics. Although the curves of the Kuz–Ram model did not differ much from each other because the blasting planes of Tests 1–4 were very similar, the conventional blasting curve was different from the others, with large sizes for different P(x). In the PortaMetrics particle size distribution curves, the values measured in the field were different for each blasting performed. Despite the small differences in each of the blasting designs, some deviations could be accounted for, such as the drilling operating conditions [8], explosive energy control [8–10], geomechanical characteristics of the rock massif [10], experimental errors of the image sampler, errors in the delineation of the rock limits and, consequently, of the size of the fragments, and errors of the FMAI algorithm.

The distributions presented in Figure 5 correspond to the validation and difference between the average sizes obtained in the determining conditions via Kuz–Ram analysis (mathematical model), and the physical analysis obtained at the place where the events were held (obtained via MMpro). It is possible to observe through the graph analyzed that despite the Kuz–Ram model being widely used in most bibliographies, this method presents a certain delimitation, making visible the inability to demonstrate the number of fine particles present in the system. In addition, the range delimited to observe the fragmentation of the grains corresponds to the granulometry to be destined for the crusher, represented in the range between 150 mm and 1200 mm. The interesting thing about checking the minimum range is related to the percentage of passers-by present in the system, and this range will be differentiated according to the blasting tests carried out.

The MMPro results showed that the material was well fragmented, with an average percentage of fragments passing through 150 mm: 69.70% for Tests 1–3; 66.20% for Test 4; and 56.4% for the conventional blasting test. Regarding the maximum sizes measured, the existence of blocks larger than 1200 mm was observed, with the exception of Test 3, where secondary mechanical blasting was indicated. As observed, the equipment detected a large amount of fines, thus making it necessary to adapt the Kuz–Ram formula, so that this material was correctly detected after fragmentation. As the ideal option after detonation is to present homogeneity between the grains and a finer range, facilitating the crushing operation, the ideal range for this to occur in is adherent to the range of 150–1200 mm. When checking the granulometric curves as a whole in Figure 5, it is possible to observe the decrease in granulometry as the tests are applied.

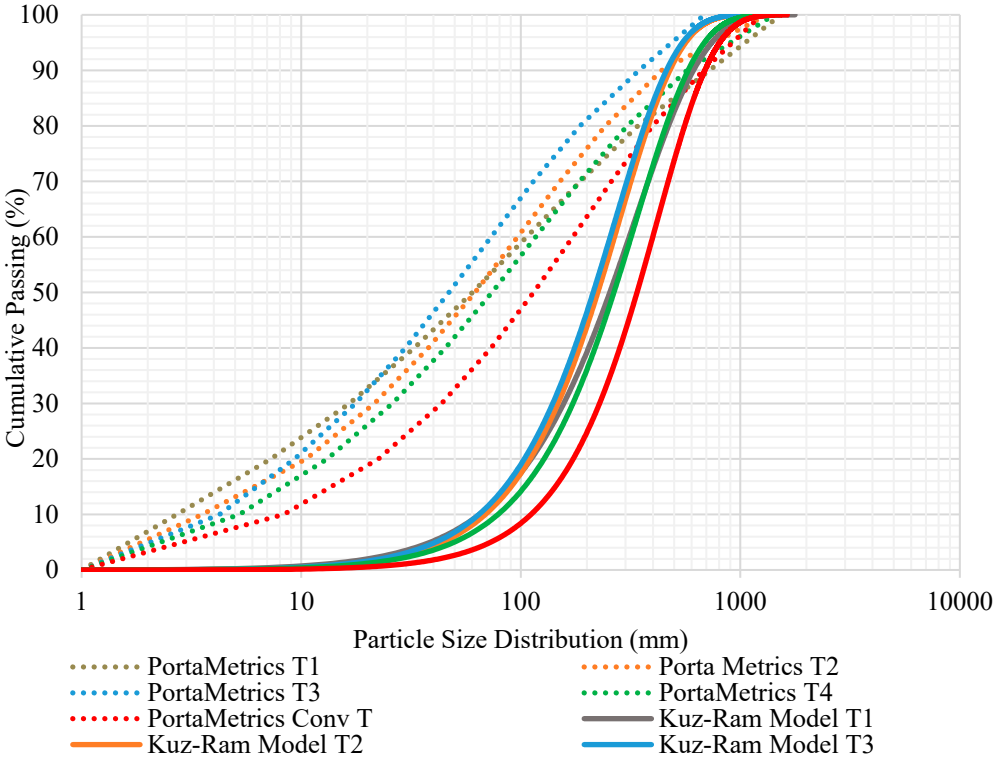

Figure 5. Kuz–Ram and MMPro particle size distributions for all tests.

When checking each test, it is verified that as the dismantling operations are configured, it is possible to obtain finer grain sizes, with a considerable gap between the Kuz–Ram curves and those generated via the grain size analysis of the equipment, checking the accuracy of the equipment. It is possible to observe that the equipment makes more superficial records and analyses of the blasting, with it not being possible to validate non-visible and overlapping particles. In order for this to have more conclusive apparent results, it is recommended to use the equipment per shell to be moved for transport, thus resulting in more accurate analyses. Even so, it is possible to observe that the proportionality of the results is maintained with the mathematical calculation, thus making it a form of significant analysis when validating the blasting.

An applied study similar to the one provided in this article can be seen by Ebrahimi [31], who used the neural network technique to optimize rock fragmentation induced by detonation. For the same to happen in this study, instead of using PortaMetrics, Split-Desktop was used, with the test verifying the same things, including a distribution variation between 15 and 40 cm, with this being possible due to using the neural network tools, a good correlation, and obtaining the rock fragmentation in an optimized way.

Based on the equations presented in Table 4 and information from Tables 2 and 5, the yield indicator related to X80 obtained in each test performed was determined to evaluate the impacts of the quality of blasting fragmentation in the subsequent operational phases. Table 6 presents the operating parameters used to calculate the yield. These parameters were obtained from a database provided by the mine, which was processed and statistically analyzed.

Figure 6a,b and Figure 7 show the productivity estimates of the loading, transport, and primary crushing phases relative to the X80 obtained in each blasting test performed in this study.

Table 6. Operating parameters used to estimate the productivity of the loading, transport, and primary crushing phases.

Parameter	Tests				
	1	2	3	4	Conventional
U_c	100.00	100.00	100.00	100.00	100.00
L_c	40.76	40.76	40.76	40.76	40.76
a	12.15	12.15	12.15	12.15	12.15
t_{sw}	21.67	21.67	21.67	21.67	21.67
t_d	3.95	3.95	3.95	3.95	3.95
U_t	100.00	100.00	100.00	100.00	100.00
L_t	243.00	243.00	243.00	243.00	243.00
p	6.00	6.00	6.00	6.00	6.00
t_v	23.62	23.62	23.62	23.62	23.62
t_f	6.38	6.38	6.38	6.38	6.38
P_{bp}	3523.00	3523.00	3523.00	3523.00	3523.00

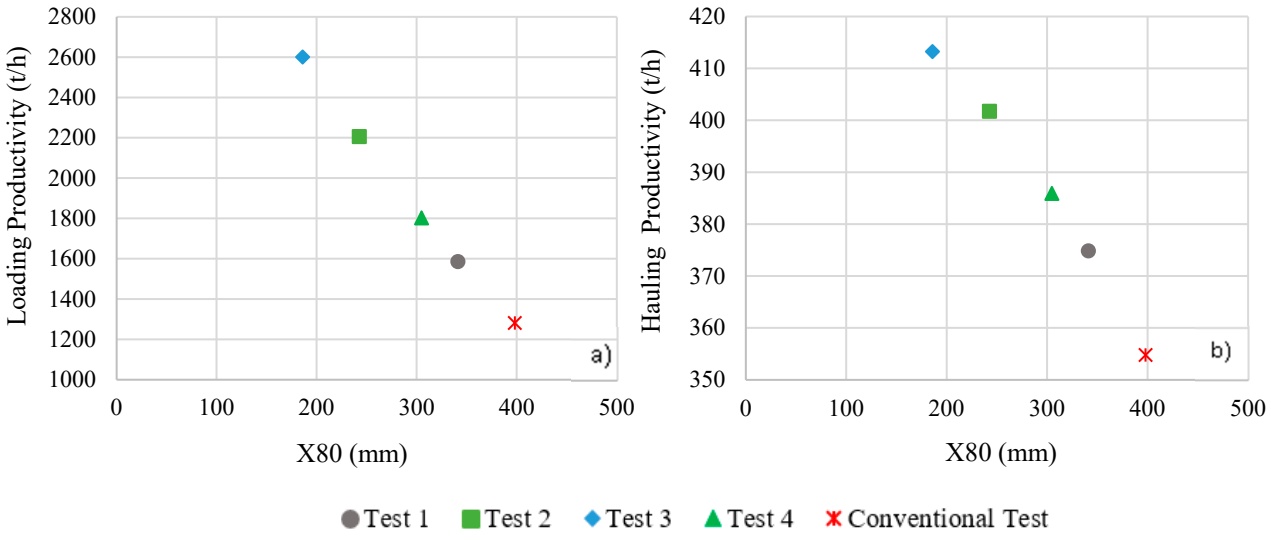

Figure 6. (**a**) Loading productivity and (**b**) transport productivity relative to X_{80}.

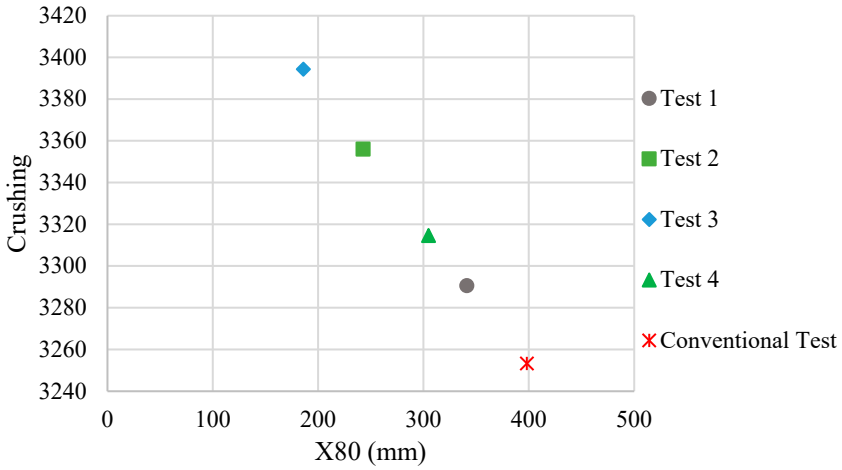

Figure 7. Primary crushing productivity relative to X_{80}.

As expected, the productivity levels of operations were inversely proportional to the sizes of the blasting fragments, specifically studied by X80 in this case. When considering each blasting and its parameters, Tests 1–4 showed a satisfactory improvement in productivity relative to conventional blasting. Because it was performed with a higher load ratio, Test

3 presented a better fragmentation result and, consequently, the best-estimated values for the productivity of the other steps. The mine productivity with conventional blasting was not the most adequate, considering the X80 obtained via the test performed in this study. However, when considering the operating costs, the maximum productivity estimated here that was related to fragmentation did not correspond to the lowest cost of any of the mine phases [32]. Some scholars have evaluated the impacts of fragmentation on productivity in loading and transport and on the energy consumption used by crushing [33]. This finding was especially true for mines with very compact ore, such as the mine under study, where there was increased pressure to improve fragmentation without significantly increasing the blasting costs [34]. What could happen when adopting the configuration of the blasting plane of Test 3, in which a greater level of explosives was used?

Based on the visual analysis in the field, it was possible to identify a relative improvement in the fragmentation of HCI. Figure 8 shows examples of images taken in each test and their respective analyses in the MMPro platform.

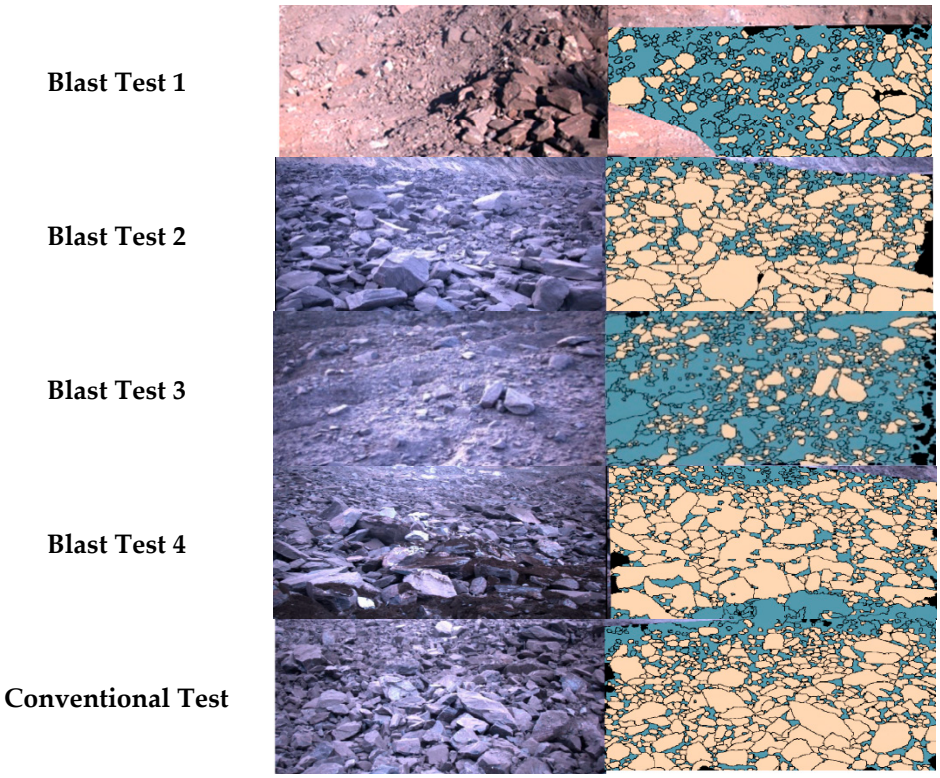

Figure 8. Examples of photographs taken from the piles of the blasting tests and graphical representation obtained using PortaMetrics™.

4. Conclusions and Recommendations

- Via the execution of blasting tests, it was possible to evaluate the quality of the fragmented material and the proposed blasting design using explosives for very compact itabirite.
- The new methodology of blasting design demonstrated compatibility with the particle size requirements of the mine, presenting a considerable reduction in X80 values.
- The comparison of the particle size distribution curves generated using PortaMetrics with the curves of the Kuz–Ram distribution model was an important method for verifying the applicability and effectiveness of the equipment.
- Through this investigation, it was possible to evaluate the productivity of the mine phases after blasting, in which the increase in the load ratio and alteration of the drilling design generated immediate results in the blasting process and, consequently, in the subsequent phases.

5. Future Works

- Using the mine to crusher methodology, it is possible to approach future work via multivariable statistical analysis and the stochastic method, transmitting in this way greater knowledge about the predictability of blasts.
- A simulation using the Monte Carlo method can also be considered, making the KPIs covered by the operations clearer and broader.
- It is also possible to evaluate other blasting parameters, such as the energy released and the amount of explosives generated, to establish optimization around this factor of interest.

Author Contributions: J.F.: Conceptualization, Methodology, Software, Validation, Formal Analysis, Investigation, Resources, Data Curation, Writing—Original Draft Preparation, Visualization, Supervision. V.T.: Conceptualization, Methodology, Validation, Visualization, Supervision, Project Administration, Funding Acquisition. R.C.: Formal Analysis, Investigation, Resources, Data Curation. D.M.: Software, Formal Analysis, Investigation, Resources, Data Curation, Writing—Original Draft Preparation, Writing—Review & Editing. All authors have read and agreed to the published version of the manuscript.

Funding: This research received no external funding.

Informed Consent Statement: Not applicable.

Data Availability Statement: The data used to create this article are confidential, it is not possible to publish them, only the graphics.

Acknowledgments: The authors would like to thank the Vale Institute of Technology and Vale SA for the material and resources used for the preparation of this study.

Conflicts of Interest: The authors declare no conflict of interest.

Ethical Statement: The authors state that the research was conducted according to ethical standards.

References

1. Nikkhah, A.; Vakylabad, A.B.; Hassanzadeh, A.; Niedoba, T.; Surowiak, A. An evaluation of the impact of ore fragmented by blasting on mining performance. *Minerals* **2022**, *12*, 258. [CrossRef]
2. Shehu, S.A.; Abdulazeez, S.; Yusuf, K.O.; Hashim, M.H.M. Comparative study of WipFrag image analysis and Kuz-Ram empirical model in granite aggregate quarry and their application for blast fragmentation rating. *Geomech. Geoeng.* **2020**, *17*, 197–205. [CrossRef]
3. Navarro Torres, V.F.; Figueiredo, J.R.; De La Hoz, R.C.; Botaro, M.; Chaves, L.S. A mine-to-crusher model to minimize costs at a truckless open-pit iron mine in Brazil. *Minerals* **2022**, *12*, 1037. [CrossRef]
4. Dumakor-Dupey, N.K.; Arya, S.; Jha, A. Advances in Blast-Induced Impact Prediction—A Review of Machine Learning Applications. *Minerals* **2021**, *11*, 601. [CrossRef]
5. Yu, Z.; Shi, X.; Zhou, J.; Chen, X.; Qiu, X. Effective Assessment of Blast-Induced Ground Vibration Using an Optimized Random Forest Model Based on a Harris Hawks Optimization Algorithm. *Appl. Sci.* **2020**, *10*, 1403. [CrossRef]
6. Al-Bkri, A.Y.; Sazid, M. Application of Artificial Neural Network (ANN) for Prediction and Optimization of Blast-Induced Impacts. *Mining* **2021**, *1*, 315–334. [CrossRef]
7. Zamora, A.N.B. *Analisis del uso de Emulsion Gasificable San-G APU para Optimizar la Fragmentaciòn de Voladuras Primarias—Compañía Minera Antamina S. A—Huaraz*; Tese para o título de Engenharia de Minas; Universidad Nacional San Antonio Abad Del Cusco: Cusco, Peru, 2019.
8. Chang, J.; Sun, L.; Dai, B.; Li, H.; Liu, Z.; Zhao, X.; Ke, B. Research on the fracture properties and mechanism of carbon dioxide blasting based on rock-like materials. *Minerals* **2023**, *13*, 3. [CrossRef]
9. Zhang, Z.X. *Rock Fracture and Blasting: Theory and Applications*; Elsevier: Amsterdam, The Netherlands, 2016.
10. Jimeno, L.C.; Jimeno, E.L.; Bermúdez, P.G. *Manual de Perforación, Explosivos y Voladura en Minería y Obras Públicas. Grupo de Proyectos de Ingeniería, ETSI Minas y Energía*; Universidad Politécnica de Madrid: Madrid, Spain, 2017.
11. Akbari, M.; Lashkaripour, G.; Bafghi, A.Y.; Ghafoori, M. Blastability evaluation for rock mass fragmentation in Iran central iron ore mines. *Int. J. Min. Sci. Technol.* **2015**, *25*, 59–66. [CrossRef]
12. Nielsen, K.; Lownds, C. Enhancement of taconite crushing and grinding through primary blasting. *Int. J. Rock Mech. Min. Sci.* **1997**, *34*, 625. [CrossRef]
13. Adel, G.; Kojovic, T.; Thornton, D. Mine-to-mill optimization of aggregate production. In *Semi-Annual Report No. 4*; Virginia Polytechnic Institute & State University: Blacksburg, VA, USA, 2006; p. 168.

14. Jethro, M.A.; Shehu, S.A.; Kayode, T.S. Effect of Fragmentation on loading at Obajana Cement Company Plc, Nigeria. *Int. J. Sci. Eng. Res.* **2016**, *7*, 608–620.
15. Taqieddin, S.A. Evaluation of the efficiency of a blasting operation designed for a dragline strip mining process. *Min. Sci. Technol.* **1989**, *8*, 59–64. [CrossRef]
16. Hamdi, E.; Du Mouza, J. A methodology for rock mass characterization and classification to improve blast results. *Int. J. Rock Mech. Min. Sci.* **2005**, *42*, 177–194. [CrossRef]
17. Kulula, M.I.; Nashongo, M.N.; Akande, J.M. Influence of blasting parameters and density of rocks on blast performance at Tschudi Mine, Tsumeb, Namibia. *J. Miner. Mater. Charact. Eng.* **2017**, *5*, 339–352. [CrossRef]
18. Khademian, A.; Bagherpour, R. Alteration of grindability of minerals due to applying different explosives in blasting operation. *Miner. Eng.* **2017**, *111*, 174–181. [CrossRef]
19. Nanda, S.; Pal, B.K. Analysis of blast fragmentation using WipFrag. *Int. J. Innov. Sci. Res. Technol.* **2020**, *5*, 1561–1566. Available online: https://ijisrt.com/assets/upload/files/IJISRT20JUN1086.pdf (accessed on 7 March 2023). [CrossRef]
20. Liu, B. Characterisation of Block Cave Mining Secondary Fragmentation. Master's Dissertation, The University of British Columbia, Vancouver, BC, Canada, 2016. Available online: https://open.library.ubc.ca/soa/cIRcle/collections/ubctheses/24/items/1.0306909 (accessed on 7 March 2023).
21. Weir, M.M. Porta Metrics. Available online: https://www.motionmetrics.com/portametrics/ (accessed on 2 February 2023).
22. Kuznetsov, V.M. The mean diameter of the fragments formed by blasting rock. *Sov. Min. Sci.* **1973**, *9*, 144–148. [CrossRef]
23. Mertuszka, P.; Kramarczyk, B.; Pytlik, M.; Szumny, M.; Jaszcz, K.; Jarosz, T. Implementation and Verification of Effectiveness of Bulk Emulsion Explosive with Improved Energetic Parameters in an Underground Mine Environment. *Energies* **2022**, *15*, 6424. [CrossRef]
24. Cunningham, C.V.B. The Kuz–Ram model for prediction of fragmentation from blasting. In Proceedings of the First International Symposium on Rock Fragmentation by Blasting, Luleå, Sweden, 23–26 August 1983; Holmberg, R., Rustan, A., Eds.; Lulea University of Technology: Luleå, Sweden, 1983; pp. 439–454.
25. Cunningham, C.V.B. Fragmentation estimations and the Kuz–Ram model—Four years on. In Proceedings of the Second International Symposium on Rock Fragmentation by Blasting, Keystone, CO, USA, 23–26 August 1987; Society for Experimental Mechanics: Bethel, CT, USA, 1987; pp. 475–487.
26. Cunningham, C.V.B. The Kuz-Ram fragmentation model—20 years on. In *Brighton Conference Proceedings*; Holmberg, R., Ed.; European Federation of Explosives Engineer: Brighton, UK, 2005; pp. 201–210.
27. Rosin, P.; Rammler, E. The law governing the fineness of powdered coal. *J. Inst. Fuel* **1933**, *7*, 29–36.
28. Amoako, R.; Jha, A.; Zhong, S. Rock Fragmentation prediction using an artificial neural network and support vector regression hybrid approach. *Mining* **2022**, *2*, 233–247. [CrossRef]
29. Hustrulid, W.A. *Blasting Principles for Open Pit Mining: Theoretical Foundations*, 1st ed.; AA Balkema: Rotterdam, The Netherlands, 1999.
30. Cameron, P.; Drinkwater, D.; Pease, J. *The ABC of Mine to Mill and Metal Price Cycles*; Australasian Institute of Mining and Metallurgy (AusIMM) Bulletin: Carlton, Australia, 2017; p. 9.
31. Mckee, D.J. *Understanding Mine to Mil*, 1st ed.; The Cooperative Research Centre for Optimizing Resource Extraction (CRC ORE): Brisbane, Australia, 2013; p. 96.
32. Varannai, B.; Johansson, D.; Schunnesson, H. Crusher to mill transportation time calculation—The Aitik case. *Minerals* **2022**, *12*, 147. [CrossRef]
33. Ebrahimi, E.; Monjezi, M.; Khalesi, M.R.; Armaghani, D.J. Prediction and optimization of back-break and rock fragmentation using an artificial neural network and a bee colony algorithm. *Bull. Eng. Geol. Environ.* **2015**, *75*, 27–36. [CrossRef]
34. Monjezi, M.; Rezaei, M.; Yazdian Varjani, A. Prediction of rock fragmentation due to blasting in Gol-E-Gohar iron mine using fuzzy logic. *Int. J. Rock Mech. Min. Sci.* **2009**, *46*, 1273–1280. [CrossRef]